Onboard Train Localization Based on Railway Track Irregularity Matching

Yukun Zhou, Qijin Chen, Rongsheng Wang, Guiliang Jia, and Xiaoji Niu

***Abstract*— Train localization is a task of fundamental importance to provide reliable and accurate train positioning information for railway control and operation. Determining the train's position using onboard sensors is a technical trend in this field. In this research, we proposed a train positioning approach by matching a new kind of rail feature, that is, track irregularity. By using an onboard inertial navigation system (INS), continuous and location-dependent track irregularity can be sensed, and then, this signal measurement is matched up to the predefined track irregularity map to locate the train. Train-borne experiments were carried out to validate the feasibility and evaluate the navigation performance of the proposed method. The results show that 0.6-m positioning accuracy with 97.26% confidence can be achieved when using a typical tactical grade inertial measurement unit (IMU), and the accuracy is 0.8 m with 95.39% confidence for a low-cost microelectromechanical system (MEMS) IMU. The proposed method is proven to be able to enhance the robustness and accuracy of the multisensory train positioning system.**

***Index Terms*— Feature matching, onboard positioning system, track irregularity, train localization.**

I. Introduction

TRAIN localization system plays a fundamental role in railway control systems, providing reliable, and accurate train positions to ensure critical safety in railway networks. Therefore, it is necessary to obtain real-time, reliable, precise information on train position for train safety and control, collision avoidance systems, and autonomous train driving systems [1]–[5].

There are many methods for train positioning, but most of them rely on trackside equipment. Trackside infrastructure elements, such as balises, track circuits, and axle counters, are used to obtain the present train location on the railway track and determine whether a certain track segment is free. However, it is relatively cost-consuming to afford the extensive amount of trackside equipment during the operation and maintenance of the railway [2], [6]. With the rapid development of positioning sensors, onboard train navigation technology has become possible and has attracted research interest [7]. Common approaches for onboard train localization include the global satellite navigation system (GNSS), the inertial navigation system (INS), the odometer, the Doppler radar, and the vision-based positioning system [3], [6], [8], [9]. Damy [6] evaluated the performance of GNSS in train localization and applied weighting techniques to mitigate the effect of multipath on train positioning. Cai *et al.* [10] introduced the accuracy, integrity, reliability, availability, and safety characteristics for GNSS-based train positioning and related evaluation methods. In the literature [2], GNSS worked as a positioning sensor for train navigation, and the results showed that GNSS is suitable for railway localization.

Since GNSS signals are easily interfered with by bridges or tunnels, multisensory positioning technology was used for train localization. Otegui *et al.* [9] proposed a train navigation methodology, which fused the GNSS and INS measurements, and achieved encouraging results. Jiang *et al.* [3], [11] proposed a train positioning method based on GNSS, INS, odometer, and map-matching (MM). When GNSS signals were unavailable, the system changed to the integration mode of INS/odometer with the assistance of the MM method. Jiang *et al.* [1] proposed a triple-integration system, which fused GNSS, INS, and optical velocity sensor (OVS) measurements for train positioning. Compared to the traditional odometer, velocity measurements from OVS are not affected by wheel idling and skidding. However, the disadvantage of this sensor combination was that it cannot maintain high navigation accuracy when GNSS signals were blocked for a long time. To improve the robustness of the navigation system in GNSS-challenging environments, Jiang *et al.* [12] attempted to use light detection and ranging (LiDAR) equipment to identify turnout frogs. The precise position of the detected turnout frog was integrated with INS to control INS divergence. Wang *et al.* [7] proposed a train localization method that integrated millimeter-wave radar and vision data. The radar provided velocity measurements and the loop closure detection technology eliminated the cumulative position error when the train achieved key location detection on the railway line.

Currently, feature matching techniques have gradually been applied to aid onboard train positioning systems to achieve higher levels of positioning performance. These localization methods determine train position in the railway network by measuring track features and comparing them with a predefined database. Saab [13], [14] attempted to achieve train

Manuscript received December 11, 2021; accepted January 5, 2022. Date of publication January 18, 2022; date of current version February 25, 2022. This work was supported in part by the National Natural Science Foundation of China under Grant 41904019 and Grant 41674038. The Associate Editor coordinating the review process was Huang-Chen Lee. *(Corresponding authors: Qijin Chen; Xiaoji Niu.)*

Yukun Zhou, Qijin Chen, and Xiaoji Niu are with the GNSS Research Center, Wuhan University, Wuhan 430072, China (e-mail: chenqijin@whu.edu.cn; xjniu@whu.edu.cn).

Rongsheng Wang and Guiliang Jia are with Fuyang Public Works Station, China Railway Shanghai Group Company, Ltd., Fuyang 236000, China.

Digital Object Identifier 10.1109/TIM.2022.3144207

positioning based on map matching. The core of his method was correlating the track segment angular rate extracted from a known map to the corresponding measurements from the onboard gyroscope. However, when the train was running in a straight section, effective matching could not be achieved. Harada *et al.* [15] proposed a train localization method that determines the train position by calculating the correlation of the track curvature characteristics between the database and the onboard equipment measurements. Gerlach and Rahmig [16] attempted to identify track switches by comparing multiple sensor outputs to a reference map. In [17] and [18], track geometric parameters, including curvature, vertical slope, and back change, were used for feature matching to increase the robustness of train positioning. In the track network, these features mentioned above for matching are usually distributed with a long-distance interval, in which case we seldom have the matching opportunity, i.e., the matching and correction only perform at low frequency. To improve rail-based localization in a tunnel, Daoust *et al.* [19] used a LiDAR sensor to record the tunnel pathological characteristics for feature matching. In addition, the distortions of the Earth's magnetic field have characteristic attributes at the same location along the railway track. These distortions have the potential for train location [20]. Hedberg and Hammar [21] and Siebler [22] introduced a train positioning method by correlating the magnetic signatures extracted from the database to the corresponding magnetic measurements.

Heirich [23], [24] pointed out that any measurable signal containing location-dependent information has the potential to aid the train localization system, whose research inspired us to carry out the present work. In this article, a new kind of railway track feature, i.e., track irregularity, is applied for matching to provide train position information. Due to the frequent passage of heavy trains and deformation of the track bed, railway track condition deteriorates and drifts away from its designed geometry, leading to track irregularity. Track irregularities are defined as the deviation from the track-designed geometry, including gauge, cross-level, alignment, and longitudinal irregularity parameters. Illustrative sketches of different types of track geometric parameters are shown in Fig. 1. For railway maintenance, track irregularity is a harmful feature for the passengers' comfort and train operation safety [25], [26]. However, from another perspective, track irregularity is a kind of location-dependent and distinctive signal that would benefit the train's localization process. Similar to the work done in [27] and [28] where the road terrain and pavement roughness characteristics were considered for vehicle localization, we demonstrate the use of railway track irregularity for train positioning. Our previous works concentrated on track irregularity surveying based on aid INS. In the literature [29], we found that railway track irregularity measurements of the same rail section have good repeatability. Meanwhile, these track irregularities in the same track mileage change very slowly during train operation, which shows their potential in train localization applications [29], [30]. Since track irregularities exist at all locations along the railway track, and they have continuous and location-dependent signatures, these irregularities can be regarded as one unique track signal for feature matching. It is possible to estimate a train position from a comparison of the latest measured signatures and reference signatures from a map. These continuous track irregularities are used as an effective matching feature to obtain accurate, continuous, and reliable train location solutions in the track network. This train localization method based on track irregularity matching is introduced in detail in the following sections.

This article makes two contributions. First, a new kind of railway track feature, i.e., track irregularity, is proposed for train localization applications. Second, an onboard INS aided by track irregularity matching can achieve accurate and self-contained positioning performance, which is not easily influenced by external disturbance. The proposed approach is proven to be able to enhance the existing onboard multisensory train positioning system and provides the researchers in this field with a new clue for solving the train localization problem.

The remainder of this article is organized as follows. Section II introduces the principles of track irregularity feature matching for train localization. Section III presents the algorithm of track irregularity matching and the Kalman filter design for the INS aided by track irregularity matching. Section IV concentrates on the experimental description and detailed accuracy assessment. Concluding remarks are summarized in Section V.

II. Principle of Track Irregularity-Based Train Localization

Train localization is an issue to determine the linear distance that a train has traveled along the track. The goal of train localization is to estimate the train longitudinal position in a specific track network [5]. During the movement of the train, an INS mounted in a train cabin provides inertial navigation positioning information for global matching search. Meanwhile, track irregularity measurement from INS works as the track feature and is matched with a predefined background map to determine the optimal train position and update the INS.

A. Railway Track Irregularity Features

1) Track Irregularity Characteristics: Track irregularities are defined as railway track drifts away from its designed geometric position and smoothness, including gauge, cross-level, alignment, and longitudinal irregularity parameters [29]. As shown in Fig. 1, alignment and longitudinal irregularities refer to the rail deviation from the track-designed line in the transverse and vertical directions. Cant refers to the difference between the elevations of the two rails, and cross-level irregularity is the difference of the real cant from the designed value [30]. Since track can be regarded as a 3-D curve, track irregularities should be expressed as the relative deviation from their nominal smoothness.

Track irregularity surveying is a problem of measuring the geometric shape of the track. When a train is running on the track, its motion trajectory, attitude angles, and changes in attitude angles are constrained by the track irregularity. Once there is any irregularity along the track, an onboard INS can sense this track excursion [31]. The essence of track

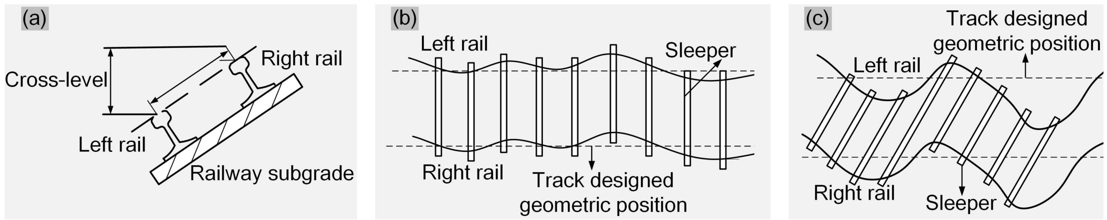

Fig. 1. Schematic diagrams of (a) cross-level, (b) alignment irregularity, and (c) longitudinal irregularity.

irregularity parameter calculation is to reconstruct the 3-D track geometry based on INS measurements. Once the actual track geometry is reconstructed, track geometric parameters and deformation can be identified, and track irregularity can be obtained. With the track attitude measurements from the onboard inertial sensor, track parameters can be reconstructed, and track irregularities can be calculated. Typically, inertial sensors, such as gyroscopes and accelerometers or INS, are mounted on the rigid structures of the train, such as the axle box, bogie, and car body to detect the cross-level, alignment, and longitudinal track irregularities. Onboard inertial sensors are field-proven robust and cost-effective methods to measure track specific irregularities [32], [33].

For feature matching localization, track irregularity features show location-dependent, continuous, and distinctive characteristics, and these track irregularities exist at all locations along the railway track. Multiple track irregularity measurements of the same track section have good repeatability, as shown in Fig. 2. According to the long-term history data from track inspection cars, track irregularity in the same track mileage changes very slowly during train operation [25]. Meanwhile, onboard inertial sensors can recognize irregularity changes, while the train moves on the line every day. These trains can be regarded as volunteers, and the measurements from onboard sensors on a daily basis are the crowd-sourced data, which reflects the change in track irregularity. These track irregularities have the potential to be updated in time based on crowd-sourced technology, which is defined as getting work done by a crowd of people, i.e., corresponds to any collective and collaborative activity performed by a large number of volunteers. Therefore, track irregularity can be regarded as a valuable positioning source for train localization.

2) Correlation Between the Irregularity and Attitude Responses: For track alignment irregularity parameter calculation, the lateral deviation is related to the shape of the railway track, and the track heading deviation indicates the tangential angles of the lateral deviation. The lateral deviation is reflected by an integral transformation of the heading deviation value. Cross-level and longitudinal irregularities are similar principle as alignment irregularity except that they use roll and pitch information, respectively. Zhu *et al.* [31] investigated the relationship between attitude angles and track irregularities in detail. They concluded that the alignment irregularity, namely, the lateral projection of the difference between the measuring value and its designed value, is determined by the heading angle value, while the longitudinal irregularity, i.e., the vertical deviation, can be indicated by the track pitch value. Similarly,

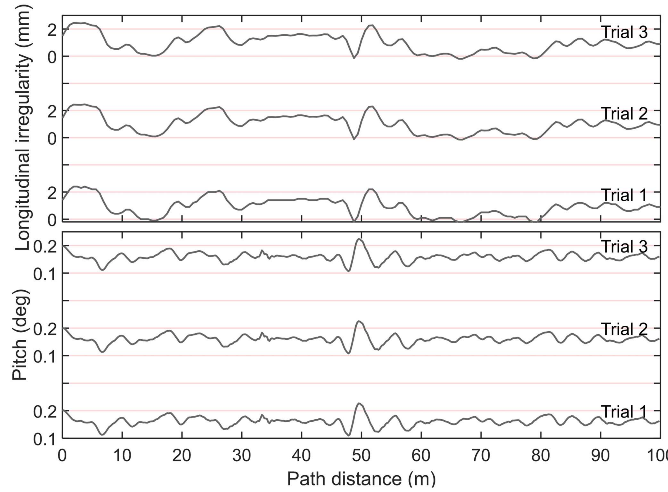

Fig. 2. Multiple measurements of the longitudinal irregularity and pitch angle on the same track show good repeatability. Longitudinal irregularity (top) correlates strongly to the pitch angle (bottom).

the roll angle reflects the difference between the elevations of the two rails according to which the cant deviation (cross-level irregularity) can be detected. Therefore, the essence of track irregularity is the change of angular value, and this irregularity can be indicated by measuring track attitude, whose principle is similar to the road roughness detection [34]. Dean *et al.* [27], [28] attempted to achieve vehicle localization based on the vehicle attitude measurements in response to the road roughness characteristic, and their research inspired us to carry out the present work. Fig. 2 depicts that the track irregularity correlates tightly to the attitude responses of the host vehicle. Therefore, we can either choose to match the attitude response signals or the track irregularity measurements. The former requires less computation; thus, without loss of generality, we will use the attitude measurement responses to track irregularity in the following for signal matching.

3) Advantages of Railway Track Irregularity Features: According to the relevant content mentioned above, we can conclude that railway track irregularity and attitude responses to this track irregularity have location-dependent, continuous, and distinctive characteristics. Track geometry features [17], [18], including curvature, vertical slope, and back change, are usually distributed with a long-distance interval, in which case we seldom have the matching opportunity, i.e., the matching and correction only perform at low frequency, as shown in Table I. It is difficult to achieve long-term train positioning by relying only on inertial sensors. Compared with these track

TABLE I
PERFORMANCE OF RAILWAY POSITIONING SYSTEMS BASED ON FEATURE MATCHING

Technology	Performance	Shortcoming
Angular rate matching [13], [14]	Correlating the track segment angular rate extracted from a known map	When train was running at a low speed, the signal-to-noise ratio is too small for feature matching
Track design geometry parameter matching [17], [18]	Using a particle filter in combination with the background map and onboard sensor measurements	The matching and correction perform at low frequency
Earth magnetic signature matching [21], [22]	Correlating the magnetic signatures extracted from the database	Passing trains will interrupt the magnetic localization

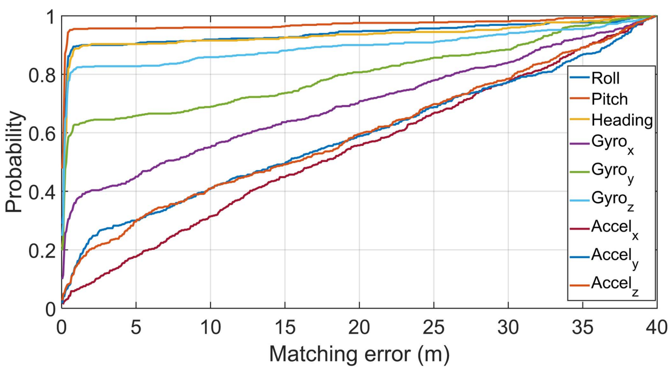

Fig. 3. CDF of the matching error by using track irregularity feature and other INS features, respectively. Roll, pitch, and heading represent the attitude measurement responses to track irregularity. Gyro$_x$, Gyro$_y$, and Gyro$_z$ are the angular rate measurements in three mutually orthogonal direction. Accel$_x$, Accel$_y$, and Accel$_z$ are the acceleration measurements in three mutually orthogonal direction.

geometry features, track irregularity has rich characteristics, which is conducive to continuous matching. Other INS features related to position information, i.e., angular rate and acceleration from onboard IMU, are tried for feature matching and train localization. We compare the matching error of using the track irregularity feature and other INS features. Fig. 3 shows that the matched position error based on angular rate or acceleration feature matching is obviously larger than that of the attitude measurement responses to track irregularity. Due to the noise of the gyro and accelerometer's original output noise, these INS features are not as suitable for matching as track irregularity. Angular rate and acceleration measurements are more sensitive to train speed. When the train runs at different speeds, the matching positioning result is not ideal. Therefore, we choose the railway track irregularity feature as the valuable signal for matching and train positioning.

B. Railway Track Irregularity Map

For the present research, the background map is defined containing geodetic coordinate pos, i.e., latitude, longitude, and height, track identification ID, mileage s, and track irregularities or the corresponding attitude angles att. Each track has an origin and a direction dir, indicating whether a train is oriented with or against the track definition. The attitude signature response to track irregularity is used as the track geometric information in the background map. These track features consist of roll, pitch, and heading angle values, which are parameterized by the 1-D position (track mileage) and stored in track points. By assigning location information to the attitude value, the track feature map consists of location-dependent correlations of the track attitude measurements. In practice, the feature map is organized by a list of continuous track points, and each point contains track ID, and the geographic and geometric track data

$$\text{map} = \{\text{ID}, s, \text{dir}, \text{pos}, \text{att}\}. \tag{1}$$

For feature matching, the background map is the foundation. There are two key points on the map: the creation of the initial map and the map update with time. In the present research, we briefly introduce how to create the initial map and how to update the map. A detailed discussion is not the focus of this article and will be sketched in future research.

For map creation and update, geometric track data, i.e., attitude signature response to track irregularity, are obtained from onboard INS. The geographic data corresponding to these attitude signatures are collected from the multisensory train positioning system, such as GNSS/INS integration, odometer, and other available sensors. In addition, the railway track geometry precise measuring results for railway construction and maintenance can be used for map creation. In future work, more types of map creation and update methods, such as crowd-sourced databases and simultaneous localization and mapping (SLAM), will be explored for field applications.

C. INS Aided by Irregularity Matching-Based Positioning

The train localization based on INS aided by irregularity matching is mainly based on INS dead reckoning and feature matching to determine accurate train position. While the train is traveling along the track, onboard INS surveys the train attitude as a feature vector to search for train location in the predefined background map continuously based on sliding window matching, as illustrated in Fig. 4. Then, this matched position can prevent inertial solution drifting. This architecture can provide a continuous and complete navigation solution.

In this article, INS works as the core sensor for train positioning. INS is a typical dead-reckoning navigation system, comprising an inertial measurement unit (IMU) and a navigation processor. The IMU usually comprises three mutually orthogonal accelerometers and three gyroscopes [35], [36]. The navigation processor integrates the IMU outputs

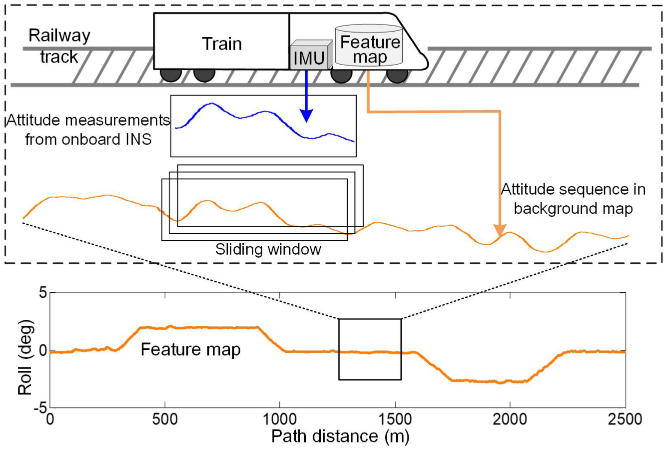

Fig. 4. Feature matching process based on attitude measurements approaches to determining train matched position along the track. Sliding window matching is used for the matched location with maximum similarity.

to give the position, velocity, and attitude. Here, INS has two main functions. In the coarse positioning and data fusion parts, INS calculates a coarse position for the optimal estimate of train localization. In the feature matching procedure, INS provides an accurate track attitude feature for the spatial signal matching process. In return, this matched position works as an external position update to compensate for INS accumulation errors in the data fusion procedure.

III. Positioning Algorithm

The train localization based on INS aided by irregularity matching is mainly divided into three phases: INS dead reckoning, feature matching, and data fusion, as shown in Fig. 5. In the INS dead reckoning phase, onboard INS produces a 3-D measurement of acceleration and angular rate. Based on the INS mechanization algorithm, short-term extremely high-accuracy navigation solutions can be obtained. These inertial navigation positions and attitudes work as track feature sequences for global matching search and local feature matching. Meanwhile, the position solution based on INS dead reckoning is defined as the coarse position of the proposed localization method. Due to the degradation in navigation accuracy with time, the error of this coarse position from INS will drift, and this coarse position error needs to be corrected by using the matched position as external observation information.

In the feature matching phase, track feature measurement, i.e., INS attitude measurement responses to track irregularity, is matched with a predefined background map to obtain the train position. First, the INS position is used for a coarse global matching search. Second, as the signature is a kind of spatial map containing information of the attitude feature along the tracks, the INS attitude solution for feature matching needs to be parameterized by distance. After spatial resampling, the INS attitude sequence works as a unique reference signature sequence for local feature matching by comparing it with the background map.

In the data fusion phase, the integration algorithm compares the inertial navigation solution with the matched position from the background map and estimates corrections to the inertial position, velocity, and attitude solution based on a Kalman filter. In this integrated navigation system, the matched position prevents inertial solution drifting, while the INS provides coarse location and track signature sequence for feature matching. This architecture can provide a continuous and complete navigation solution with high long- and short-term accuracies.

During the INS calculation and integrated navigation process, many reference frames are involved, including the inertial frame, the navigation frame, the Earth frame, the body frame, the computer frame, and the vehicle frame. The definition of these reference frames and the relationships between them are introduced in the literature [37]. In this article, the axis directions of the body frame and navigation frame are defined as the forward–bottom–right system and the north–east–down system, respectively.

A. INS Dead Reckoning

In the INS dead reckoning procedure, we apply the INS mechanization algorithm to calculate INS navigation solutions. INS mechanization refers to the procedure of updating navigation results through IMU outputs, which integrates the IMU outputs to produce a position, velocity, and attitude solution. Each INS mechanization process uses the previous navigation solution as its starting point. Therefore, at the beginning of the whole localization process, the navigation solution must be initialized, as shown in Fig. 5. In this article, if train positioning starts in the station, the initial position can be obtained from the track design document or landmark. According to this position information, the background feature map will provide the initial attitude to complete inertial navigation initialization. If the train is running on the line at the beginning, in-motion alignment techniques are used during the initialization phase [37]–[39]. INS mechanization comprises three steps: velocity update, position update, and attitude update. We can obtain the inertial navigation solutions by solving the local-navigation-frame navigation equations, which are expressed as [37]

$$\begin{bmatrix} \dot{\boldsymbol{v}}^n \\ \dot{\mathbf{C}}_n^e \\ \dot{h} \\ \dot{\mathbf{C}}_b^n \end{bmatrix} = \begin{bmatrix} \mathbf{C}_b^n \boldsymbol{f}^b - \left(2\boldsymbol{\omega}_{ie}^n + \boldsymbol{\omega}_{en}^n\right) \times \boldsymbol{v}^n + \boldsymbol{g}_l^n \\ \mathbf{C}_n^e \left(\boldsymbol{\omega}_{en}^n \times\right) \\ -v_D \\ \mathbf{C}_b^n \left(\boldsymbol{\omega}_{ib}^b \times\right) - \left(\boldsymbol{\omega}_{in}^n \times\right) \mathbf{C}_b^n \end{bmatrix} \tag{2}$$

where $\boldsymbol{v}^n$ shows the velocity in the local navigation frame (n-frame). $\mathbf{C}_b^n$ expresses the body frame (b-frame) to the n-frame coordinate transformation matrix. $\boldsymbol{f}^b$ and $\boldsymbol{\omega}_{ib}^b$ represent the outputs from accelerometers and gyros, respectively. $\boldsymbol{\omega}_{ie}^n$ is the Earth angular rate vector in the n-frame. $\boldsymbol{\omega}_{en}^n$ is the angular rate of the n-frame with respect to the e-frame resolved in the n-frame. $\boldsymbol{g}_l^n$ refers to the local gravity. $\mathbf{C}_n^e$ is the n-frame to the e-frame transformation matrix, which shows the position of vehicle. The geodetic longitude and latitude can be calculated from $\mathbf{C}_n^e$. h is the geodetic height. v_D refers to the downward velocity in the n-frame. $\boldsymbol{\omega}_{in}^n$ is the angular rate of the n-frame relative to the inertial frame (i-frame) in the n-frame.

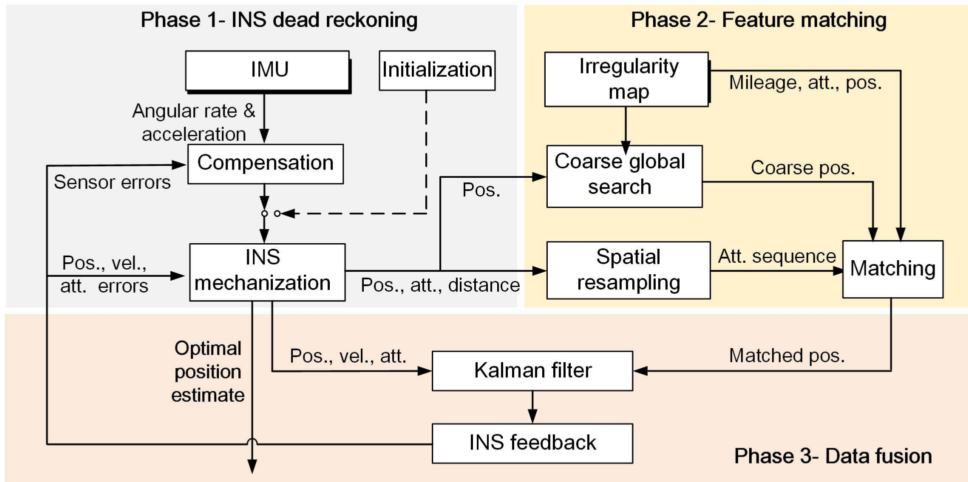

Fig. 5. Basic data processing schematic of onboard train localization based on attitude feature matching.

INS can provide short-term high-accuracy navigation solutions for train location and attitude feature matching. Due to the accumulation of IMU output errors, INS cannot maintain high-accuracy measurements for long-term periods, and the error of position solutions will drift without efficient correction from external position updates [40]. Therefore, matched positioning information works as the external observation to compensate for IMU errors and provide optimal location results.

In the INS dead reckoning procedure, INS provides short-term extremely high-accuracy navigation solutions for feature matching. This matched position works as external observation information to correct INS drift errors. In our positioning method, since INS can be continuously corrected in the integrated navigation system, the INS dead reckoning module does not need to maintain high precision for a long time. Meanwhile, we use typical tactical-grade IMU and MEMS as the measuring sensors, and the IMU measurement error is larger than that of high-precision navigation grade IMU. For the state-of-the-art INS dead reckoning approaches [41]–[43], our sensor output error is far greater than the calculation error from the traditional algorithm itself. Compared with the conventional INS dead reckoning algorithm, the state-of-the-art inertial navigation algorithm is unnecessary. Therefore, we use a classical INS mechanization algorithm for inertial navigation calculation.

B. Feature Matching

Once we obtain the coarse position from INS at a global scale, the accurate local matching phase is initiated. The current position and attitude estimates for feature matching are determined from INS solutions. Compared with the predefined background map, we can obtain the train location. Sequence matching comprises three steps: transformation to the spatial domain, spatial resampling, and similarity measuring.

1) Transformation to Spatial Domain: As the signature is to be a kind of spatial map containing attitude information along the tracks, the signal needs to be parameterized by distance instead of time. By using the Gauss–Kruger projection [40], the distance information corresponding to INS attitude solutions can be calculated

$$\Delta s = \sqrt{\Delta {r_N}^2 + \Delta {r_E}^2} \tag{3}$$

where r_N and r_E are the INS-indicated north and east coordinate components from the Gauss–Kruger projection, respectively. s is the train mileage corresponding to INS attitude measurements.

2) Spatial Resampling: To facilitate processing, it is desirable to have a uniformly sampled signal, so the next step is to resample the spatial transformed signal to obtain constant spatial sampling rate. An equal distance interval resampling is implemented on the mileage sequence (s, t), and the resampling step is expressed as d. A simple moving average is applied to the corresponding measurement series of attitude and position to resample them at a fixed distance interval d and smooth out the short-term fluctuation or the high-frequency noise [29]. The corresponding INS attitude sequence in space $\{s,\ \text{att}\}$ can be expressed as

$$\{s,\ \text{att}\} = \left\{(s_0 + d, a_1), (s_0 + 2d, a_2), \cdots, \left(s_0 + nd, a_n\right)\right\} \tag{4}$$

where $\{s,\ \text{att}\}$ expresses the whole spatial resampled attitude sequence, including the attitude signal and corresponding mileage information. s_0 is the start mileage of the sequence. d is the distance between the adjacent points (also known as the resampling interval of the attitude sequence). a represents the attitude value of each point along the whole spatial sequence. $(s_0 + nd, a_n)$ is the endpoint of the spatial sequence.

3) Similarity Measuring: After spatial resampling, signal similarity measuring is used to determine the optimal matched position on the background map. The following data processing procedure is described as follows.

(1) Determine the search range in the global background map based on the INS position solution, as shown in Fig. 2.
(2) Calculate the Pearson correlation coefficient of the query sequence and the map sequence.
(3) Shift the map sequence by one sampling distance interval.

(4) Repeat steps 2 and 3 until the end of the search area has been reached.
(5) Select the maximum Pearson correlation coefficient for the current query sequence, and determine the longitudinal position from the map related to this maximum correlation coefficient.

The Pearson correlation coefficient between two sequences can be expressed as

$$r_{xy} = \frac{\sum_{i=1}^{m}(x_i - \bar{x})(y_i - \bar{y})}{\sqrt{\sum_{i=1}^{m}(x_i - \bar{x})^2}\sqrt{\sum_{i=1}^{m}(y_i - \bar{y})^2}} \tag{5}$$

where x and y represent two sequences. r_{xy} is the Pearson correlation coefficient between these two sequences, and m is the sample size. $\bar{x}$ and $\bar{y}$ are the mean values of these two sequences. In this part, x is the attitude feature sequence from INS solution, and y is the attitude feature sequence from the background map.

C. Data Fusion

After attitude sequence matching, the matched position from the background map works as an external position observation to compensate for INS accumulation errors in a loosely coupled architecture, as shown in Fig. 5.

1) System Models: In this section, a state propagation model is developed for a Kalman filter estimating position, velocity, and attitude errors resolved in the local navigation frame (n-frame), together with the biases and scale factor of the accelerometer and gyro [37], [40], [44], [45]. The error state vector of KF is defined as

$$\boldsymbol{x}(t) = \left[\, (\delta\boldsymbol{r}^n)^{\mathrm{T}} \;\; (\delta\boldsymbol{v}^n)^{\mathrm{T}} \;\; \boldsymbol{\phi}^{\mathrm{T}} \;\; \boldsymbol{b}_g{}^{\mathrm{T}} \;\; \boldsymbol{b}_a{}^{\mathrm{T}} \;\; \boldsymbol{s}_g{}^{\mathrm{T}} \;\; \boldsymbol{s}_a{}^{\mathrm{T}} \,\right]^{\mathrm{T}}. \tag{6}$$

In this definition, δ expresses the error of a variable. $\delta\boldsymbol{r}^n = [\delta r_N \;\; \delta r_E \;\; \delta r_D]^{\mathrm{T}}$ and $\delta\boldsymbol{v}^n = [\delta v_N \;\; \delta v_E \;\; \delta v_D]^{\mathrm{T}}$ are the INS-indicated position and velocity error resolved in the n-frame, respectively, and we define $\delta\, h = -\delta r_D$. $\boldsymbol{\phi} = [\phi_{\text{roll}} \;\; \phi_{\text{pitch}} \;\; \phi_{\text{yaw}}]^{\mathrm{T}}$ is the 3-D attitude error vector. $\boldsymbol{b}_g$ and $\boldsymbol{b}_a$ represent the residual bias errors of gyros and accelerometers of IMU, respectively. $\boldsymbol{s}_g$ and $\boldsymbol{s}_a$ refer to the residual scale factor errors of gyros and accelerometers, respectively. The system state model of the Kalman filter in the continuous time is written as

$$\dot{\boldsymbol{x}}(t) = \mathbf{F}(t)\boldsymbol{x}(t) + \mathbf{G}(t)\boldsymbol{w}(t) \tag{7}$$

where $\boldsymbol{x}$ is the state vector. $\mathbf{F}$ denotes the system matrix describing the system dynamics. $\mathbf{G}$ is the system noise distribution matrix. $\boldsymbol{w}$ refers to the system noise vector. To obtain the aided INS system model, time derivative of each state variable must be calculated. The position, velocity, and attitude error differential equations are

$$\begin{aligned}\delta\dot{\boldsymbol{r}}^n &= -\boldsymbol{\omega}_{en}^n \times \delta\boldsymbol{r}^n + \delta\boldsymbol{\theta} \times \boldsymbol{v}^n + \delta\boldsymbol{v}^n \\ \delta\dot{\boldsymbol{v}}^n &= \mathbf{C}_b^n\delta\boldsymbol{f}^b + \mathbf{C}_b^n\boldsymbol{f}^b \times \boldsymbol{\phi} - \left(2\boldsymbol{\omega}_{ie}^n + \boldsymbol{\omega}_{en}^n\right) \times \delta\boldsymbol{v}^n \\ &\quad + \boldsymbol{v}^n \times \left(2\delta\boldsymbol{\omega}_{ie}^n + \delta\boldsymbol{\omega}_{en}^n\right) + \delta\boldsymbol{g}_l^n \\ \dot{\boldsymbol{\phi}} &= -\boldsymbol{\omega}_{in}^n \times \boldsymbol{\phi} + \delta\boldsymbol{\omega}_{in}^n - \mathbf{C}_b^n\delta\boldsymbol{\omega}_{ib}^b\end{aligned} \tag{8}$$

where $\delta\boldsymbol{\theta} = [\delta\lambda\cos\varphi \;\; -\delta\varphi \;\; \delta\lambda\sin\varphi]^{\mathrm{T}}$, λ denotes latitude, and $\delta\lambda$ and $\delta\varphi$ are errors of latitude and longitude, respectively. $\delta\boldsymbol{f}^b$ is the error of the specific force vector resolved in the b-frame, and $\delta\boldsymbol{\omega}_{ib}^b$ refers to the error of gyro output. $\delta\boldsymbol{\omega}_{ie}^n$, $\delta\boldsymbol{\omega}_{en}^n$, and $\delta\boldsymbol{\omega}_{in}^n$ are the errors of $\boldsymbol{\omega}_{ie}^n$, $\boldsymbol{\omega}_{en}^n$, and $\boldsymbol{\omega}_{in}^n$, respectively. The details of the error differential equations can be found in the literature [37].

To be included in the state vector, the inertial sensor errors must be modeled. A stationary Gaussian process that has an exponentially decaying autocorrelation is called a first-order Gauss–Markov process. The first-order Gauss–Markov process fits a large number of physical processes with reasonable accuracy and can represent bounded uncertainty, which is the most outstanding characteristic of the first-order Gauss–Markov process. Hence, the first-order Gauss–Markov process is suitable in INS filters to model slowly varying sensor errors, such as the residual biases and residual scale factors of IMU [37]. According to the characteristic of IMU outputs, the residual biases and scale factor errors of IMU gyroscopes and accelerometers are modeled as the first-order Gauss–Markov process, which can be expressed as

$$\begin{cases}\dot{\boldsymbol{b}}_g(t) = -\dfrac{1}{T_{gb}}\boldsymbol{b}_g(t) + \boldsymbol{w}_{gb}(t) \\ \dot{\boldsymbol{b}}_a(t) = -\dfrac{1}{T_{ab}}\boldsymbol{b}_a(t) + \boldsymbol{w}_{ab}(t) \\ \dot{\boldsymbol{s}}_g(t) = -\dfrac{1}{T_{gs}}\boldsymbol{s}_g(t) + \boldsymbol{w}_{gs}(t) \\ \dot{\boldsymbol{s}}_a(t) = -\dfrac{1}{T_{as}}\boldsymbol{s}_a(t) + \boldsymbol{w}_{as}(t)\end{cases} \tag{9}$$

where T_{gb}, T_{ab}, T_{gs}, and T_{as} represent the correlation time. $\boldsymbol{w}_{gb}$, $\boldsymbol{w}_{ab}$, $\boldsymbol{w}_{gs}$, and $\boldsymbol{w}_{as}$ refer to the corresponding driving white noise of strength $2\sigma/T$, where σ is the root mean square (rms) value of the process.

2) Measurement Models: During the data fusion process, the available external measurement for INS correction is the matched position from sequence matching. To reduce the influence of mismatching errors, the matched position is valid only when the difference between the INS indicated position and matched position in the longitudinal direction is less than the set threshold. The self-evaluation can be represented as

$$\Delta p_s = |s_{\text{INS}} - s_{\text{matched}}| < Th_s \tag{10}$$

where s_{INS} and s_{matched} represent the INS indicated position and matched position in the longitudinal direction, respectively. Δp_s is position difference, and Th_s is the threshold. In the Kalman filter, the system error covariance matrix, P, defines the expectation of the square of the deviation of the state vector estimate from the true value of the state vector. The diagonal elements of P are the variances of each state estimate, while their square roots are the uncertainties [38]. Here, we determine the set threshold based on the INS indicated position error uncertainty from the diagonal elements of P. From the system error covariance matrix, we can obtain the theoretic standard deviation of the INS-indicated position error, including σ_{r_N} and σ_{r_E}. In practice, the theoretic standard deviation from the system error covariance matrix is less than the true value, so we set the threshold as

$$Th_s = 3 * \sqrt{\sigma_{r_N}^2 + \sigma_{r_E}^2}. \tag{11}$$

The system observation model of the Kalman filter in the continuous time can be expressed as

$$z(t) = \mathbf{H}(t)\boldsymbol{x}(t) + \boldsymbol{v}(t) \tag{12}$$

where $\mathbf{H}$ denotes the measurement matrix. $\boldsymbol{z}$ is the observation vector in the continuous time. $\boldsymbol{v}$ shows the measurement noise covariance matrix.

The measurement innovation vector comprises the difference between the matched position and the INS indicated position, and the measurement model can be expressed as

$$z_r = \left(\hat{\boldsymbol{r}}^n_{\text{INS}} - \tilde{\boldsymbol{r}}^n_{\text{matched}}\right) \tag{13}$$

where $\hat{\boldsymbol{r}}^n_{\text{INS}}$ denotes the INS indicated position. $\tilde{\boldsymbol{r}}^n_{\text{matched}}$ shows the matched position from sequence matching.

The measurement matrix in this Kalman filter can be written as

$$\mathbf{H} = \begin{bmatrix} \mathbf{I}_3 & \mathbf{0}_3 & \mathbf{0}_3 & \mathbf{0}_3 & \mathbf{0}_3 & \mathbf{0}_3 & \mathbf{0}_3 \end{bmatrix} \tag{14}$$

where $\mathbf{I}_3$ and $\mathbf{0}_3$ are the identity matrix and null matrix, respectively.

Ideally, the measurement noise covariance matrix, $\boldsymbol{v}$, should be determined based on the error covariance matrix of matched position. However, it is difficult to calculate this level of confidence in practice. The Kalman filter assumes that all measurement noise sources are white. If the measurement noise covariance tends to be more nebulous or is difficult to be separated out from system effects, an effective way is to exaggerate $\boldsymbol{v}$ in order to account for time correlation in the measurement noise [38]. In this article, the measurement noise from the matched position is assumed to be constant and modeled as Gauss white noise, which is determined by appropriately exaggerating the empirical value of the matched position error.

IV. Field Tests

A. Experiment Description

To evaluate the performance of the proposed method based on feature matching for train localization, train-borne field tests were performed on a track maintenance train, as shown in Fig. 7. In the field experiment, onboard measuring sensors were used to collect data on the Fuyang–Lu'an line, Anhui, China. IMUs were mounted inside the cabin for train localization. A typical tactical-grade IMU, POS-320, was used as the INS. POS320 is manufactured by Beijing NAV Technology Company Ltd., Beijing, China. This system contains three servo accelerometers and closed-loop fiber optic gyros to measure the continuous angular and acceleration velocities of the train in three mutually orthogonal directions. In addition, a low-cost microelectromechanical system (MEMS) module, INS-Probe, was used as the low-accuracy INS. This MEMS integrated system was developed by the Navigation Group, GNSS Research Center, Wuhan University. An MEMS IMU, ADI16465, from Analog Devices Inc. (ADI), MA, USA, was integrated into the INS-Probe. The performance specifications of POS320 and MEMS are listed in Table II.

1) IMU: POS320, a typical tactical-grade IMU; ADI16465: an MEMS IMU.

TABLE II

Specifications of the IMUs

Performance	POS320	MEMS
Gyroscope range	±300 deg/s	±250 deg/s
Gyroscope in-run bias stability	0.5 deg/h	40 deg/h
Angular random walk	0.03 deg/$\sqrt{h}$	0.1 deg/$\sqrt{h}$
Accelerometer range	±10 g	±6 g
Accelerometer in-run bias stability	25 mGal (1 mGal = 10^{-5} m/s^2)	100 mGal
Velocity random walk	0.1 m/s/$\sqrt{h}$	0.3 m/s/$\sqrt{h}$

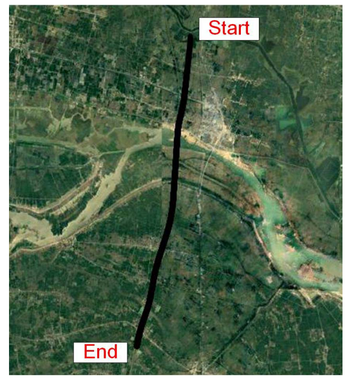

Fig. 6. Horizontal trajectory of the train-borne test on the Fuyang–Lu'an railway line.

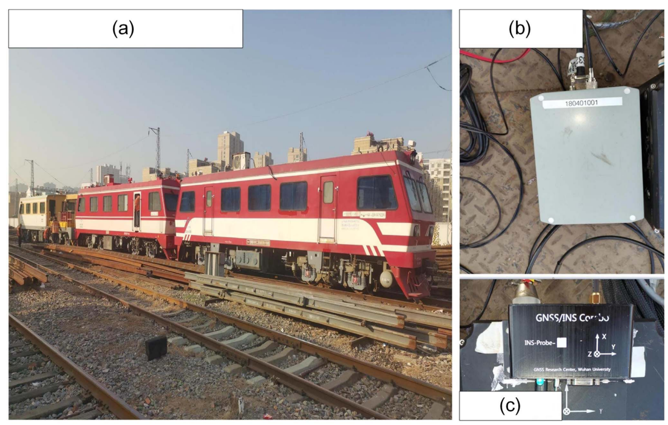

Fig. 7. Photograph of the experimental setup. (a) Maintenance train was used as the vehicle platform. (b) POS320 and (c) MEMS were mounted inside the train cabin.

2) Independent Reference: GNSS position based on the postprocessing kinematic (PPK) mode, which has centimeter-level positioning accuracy.

The running path of the train was about 12 km, as shown in Fig. 6. We did four independent train-borne tests on this path. Before the train localization test, a track feature background map with centimeter-level position accuracy was created by using GNSS and INS measurements in advance.

B. Performance Analysis

According to the data processing flow for track attitude-based localization, the experimental results are analyzed in three strategies, including the feasibility analysis of track

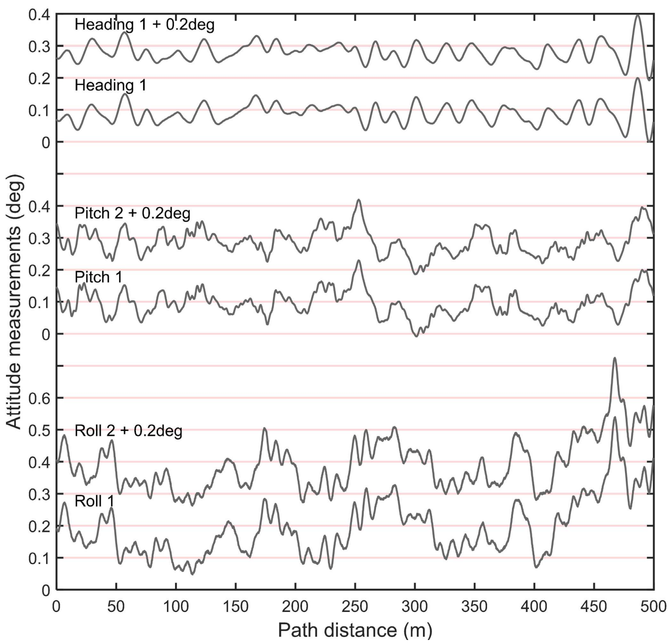

Fig. 8. Comparison of the heading (top graph), pitch (middle graph), and roll (bottom graph) angle sequences versus the distance in two runs of the same line (plotted with respect to a nominal offset for distinction purposes). POS320 provides the attitude measurements.

irregularity in train positioning, feature matching parameter analysis, and practicality and stability performances. The accuracy of this train localization method is assessed by comparing it to the reference system. In this part, we use POS320 measurements as an example for performance analysis and then repeat the analysis using the same method for the MEMS results. In the railway control system, the train position in the longitudinal direction (railway track mileage) usually works as the only position information for train safety and control. Therefore, we define that the train position in this article is the position in the longitudinal direction (railway track mileage), which can be calculated based on the train north coordinate and east coordinate. It should be noted that onboard IMU works as the only measuring sensor and participates in the real-time train localization process in this field test.

1) Feasibility Analysis of Track Irregularity in Train Positioning: Before the online positioning process, a preliminary attitude repeatability analysis is needed to evaluate the feasibility of track feature matching. We choose the measurements of two runs over the same line. Onboard INS measured the attitude of these two runs, including the roll, pitch, and heading response to the track irregularities. These attitude measurements were transformed to be a function of path distance instead of time to allow for the subsequent direct path-dependent comparison between the attitude measurements. Fig. 8 shows a typical section of the attitude responses from these two runs over the same track.

The two curves of attitude measurements in Fig. 8 appear similar in both shape and magnitude, which indicates that the real roll, pitch, and heading responses to the track irregularities have good repetition and stability over the same track section. From the plots in Fig. 8, it can be concluded that railway track attitude measurements correlate to track position. As mentioned in Section II, heading, pitch, and roll angle measurements are highly correlated with track irregularity determination, including track alignment, longitudinal, and cross-level irregularity. These plots show that the attitude measurements can reflect the real track irregularity and have the potential for train localization in track networks. These attitude responses from onboard INS, including roll, pitch, and heading measurements, have good repeatability when the train runs in the same line. It can be suggested that a train can achieve localization by correlating a previous map with attitude response history.

2) Feature Matching Parameter Analysis: For the sequence matching method, positioning accuracy is usually affected by the length of the query sequence. Here, a common question is how long it would be suitable for a query sequence to achieve reliable and high-precision matching. In this section, a statistical analysis of the positioning error is used to address this question, including the position drift error from INS mechanization, the matched position error, and the final train position error based on the optimal location estimation. It should be noted that the path distance of the query feature comes from INS position solutions. In addition, the effect of spatial resampling interval of feature map on the result is discussed in this section.

a) INS mechanization position drift error analysis: The query sequences for matching are obtained from the INS dead reckoning, as shown in Fig. 5. If the query sequence is excessively long, the INS position will drift without effective correction. The matching accuracy will start to suffer from signature distortions due to the query sequence length error from INS. Therefore, INS position drift errors in the longitudinal direction need to be evaluated using the following procedure: 1) select one query sequence length; 2) calculate the INS position drift errors in the longitudinal direction for this length; the GNSS solution based on the PPK mode works as the independent reference; 3) calculate the rms value of above INS position drift errors; and 4) repeat steps 1–3 for different query lengths.

Fig. 9(a) shows the rms value of the POS320 position drift error in the longitudinal direction versus the length of the query sequence. The train runs at a speed of about 20 m/s during the field test. This figure indicates that, when the length of the query sequence is less than 400 m, the rms value of the POS320 position error in the longitudinal direction can remain within 1 m. It is evident that the position error from INS mechanization will gradually increase as the dead-reckoning distance increases. Therefore, for feature matching, the query sequence is not the longer, the better.

b) Matching accuracy: For sequence matching, if the query sequence length is too short, the signature will not contain enough information for good localization. If it is too long, the results will start to suffer from signature distortions due to errors in the travel distance measurement, as analyzed above. We attempt to address this issue by conducting a statistical analysis of the matching success rate following the procedure described in the previous section: 1) select one query sequence length; 2) calculate the matched position errors for this length; GNSS solution based on PPK mode works as

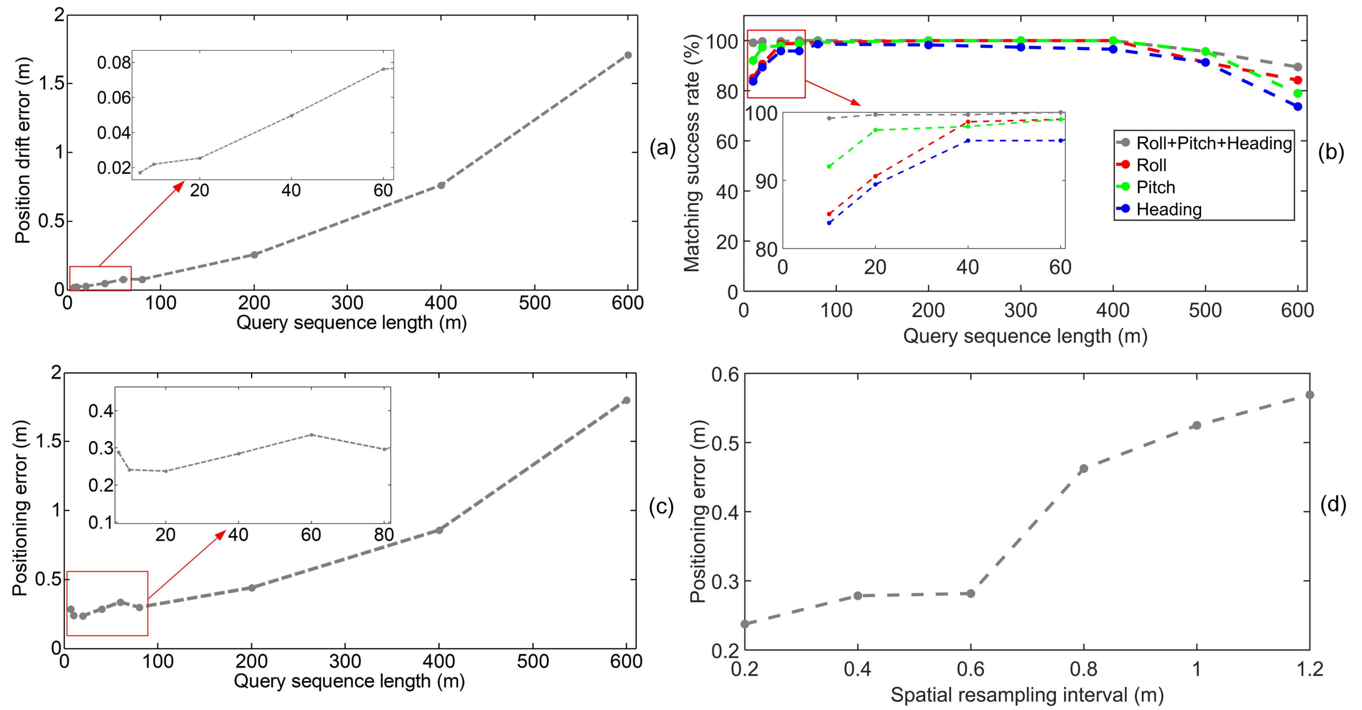

Fig. 9. RMS value of (a) INS mechanization positioning drift error, (b) matching success rate, (c) rms value of the data fusion positioning error versus the length of the query sequence, and (d) rms value of the data fusion positioning error versus the spatial resampling interval. POS320 works as the measuring and positioning sensor.

the independent reference; 3) calculate the matching success rate for this query sequence length; and 4) repeat steps 1–3 for different query lengths. In step 3, if one matched position error is less than 1 m, this point is identified as a successful matching, whose accuracy can satisfy the demand of safe railway operation [11].

Fig. 9(b) shows the matching success rate of POS320 versus the query length. The feature matching consists of roll, pitch, and heading measurements from onboard INS. This figure indicates that the matching success rate improves gradually as the length of the query sequence increases. However, the matching success rate will decrease when the query sequence is excessively long due to the increment of the travel distance measurement errors. It is noticeable in this figure that the matching success rate using the heading angle is slightly lower than those of the roll and pitch angles. Compared with pitch and roll angles, the heading angle has a lower measuring precision based on INS mechanization. Fig. 9 shows that the success rate values converge to approximately 90% for the roll, pitch, and heading angles when the query length for feature matching exceeds 20 m. If all roll, pitch, and heading measurements are used in combination for feature matching, the matching success rate can be improved effectively. It indicates that reliable and robust matching can be achieved when the query length reaches 20 m. The matching success rates using only roll, pitch, and heading responses from the POS320 system are 91%, 96%, and 89%, respectively, while the value can reach 99% when using roll, pitch, and heading responses in combination. When the train runs at a speed of about 20 m/s, the time it takes for the train to travel 20 m along the track is extremely short. INS can maintain measurement accuracy during this time, which has the ability to provide a high-precision query sequence for matching. Therefore, for a typical tactical-grade IMU, POS 320, the length of the query sequence can be set as 20 m for the feature matching and train localization processes.

c) Performance of the INS aided by matching: As illustrated in Fig. 5, the matched position is fused with the INS's solutions to obtain the optimal train's location estimates. As analyzed above, reliable and robust matching can be achieved when the query length reaches 20 m. Meanwhile, this matched position works as an external update for correcting INS accumulation errors. It can be inferred that INS aided by track irregularity matching has the ability to provide continuous and reliable train position results.

Fig. 9(c) shows the rms value of the positioning error versus query length, which is obtained using the following procedure: 1) select one query sequence length; 2) calculate the INS/feature matching integrated positioning solution; roll, pitch, and heading angles are used in combination for matching; and this positioning result is the INS/feature matching integrated solution based on optimal location estimation; 3) calculate the data fusion errors in the longitudinal direction for this length; GNSS solution based on PPK mode works as the independent reference; 4) calculate the rms value of above positioning errors; and 5) repeat steps 1–4 for different query lengths. This figure indicates that the rms value of the integrated positioning error fluctuates within the range of 0.3 m when the query sequence length is less than 80 m. If the query sequence is excessively long, the positioning error gradually increases as the query sequence length increases, which is consistent with the result of the INS mechanization position drift error analysis part and the matched position error analysis part.

d) Influence of spatial resampling interval on positioning accuracy: In Fig. 9(b) and (c), we choose 20 m as the optimal length of the query sequence for POS320 feature matching. For feature matching, we need to evaluate the impact of the sampling frequency of the query sequence, which is obtained using the following procedure: 1) determine the query sequence length as 20 m; 2) select one sampling frequency of query sequence; 3) calculate the INS/feature matching integrated positioning solution; 4) calculate the data fusion errors of POS320 in the longitudinal direction for this length; GNSS solution based on PPK mode works as the independent reference; 5) calculate the rms value of above positioning errors; and 6) repeat steps 1–5 for different sampling frequencies. Fig. 9(d) expresses the rms value of the data fusion positioning error versus the spatial resampling interval. POS320 provides the INS measurements. This positioning result is the INS/feature matching integrated solution based on optimal location estimation. From this figure, the positioning errors become larger as the spatial resampling interval increases. During the feature matching process, as the spatial resampling interval increases, the query sequence contains less information for feature matching, and matched position errors will become larger.

3) Practicality and Stability Performances:

a) Performance of MEMS IMU: To unlock the potential of the proposed train localization method for large-scale applications, we also use a low-cost IMU, MEMS module to evaluate the positioning performance. Here, we use the same steps as POS320 to determine the optimal query sequence length of MEMS for feature matching. Fig. 10 shows the rms value of the longitudinal position error from MEMS versus the length of the query sequence. The optimal query sequence length of MEMS is 15 m, which is less than that of POS320 result, i.e., 20 m, as shown in Fig. 9(c). Compared to POS320, the MEMS IMU has a larger measuring error, and its navigation error drifts faster without external correction. For the same sequence length, the positioning error of MEMS is greater than that of POS320. MEMS positioning solution deviates from the true value more quickly as the query sequence increases. Therefore, the optimal query sequence length of MEMS is less than that of POS320.

b) Repeat analysis: To test the robustness and fully evaluate the performance of the proposed positioning method based on INS aided by matching, we did four independent train-borne field tests on the Fuyang–Lu'an line, which was about 12 km. Fig. 11 shows the cumulative distribution function of the positioning errors of these four test results using POS320 and MEMS, respectively. The results indicate that a typical tactical-grade IMU, POS320, aided by matching can achieve 1-m positioning accuracy. The localization accuracy of MEMS IMU is less than 2 m during four independent tests. A meter localization accuracy with good reliability and robustness can be achieved with feature matching from track irregularity by only using an onboard INS self-contained.

To analyze the positioning errors of POS320 and MEMS more intuitively, we combine the positioning error sequences of four independent measurements and calculate its cumulative distribution function, as shown in Fig. 12. According to the specifications in Table II, the measuring precision of MEMS is much less than that of POS320. However, the localization accuracy of MEMS and POS320 solutions does not show a significant difference in performance in Fig. 12. Based on the proposed localization method, the low measuring precision of IMU does not lead to positioning accuracy decreases apparently. For a running train, the time to pass a matching window is very short. MEMS IMU can maintain high-precision navigation during this time. This navigation result is converted into feature sequences for matching. Meanwhile, the high-precision

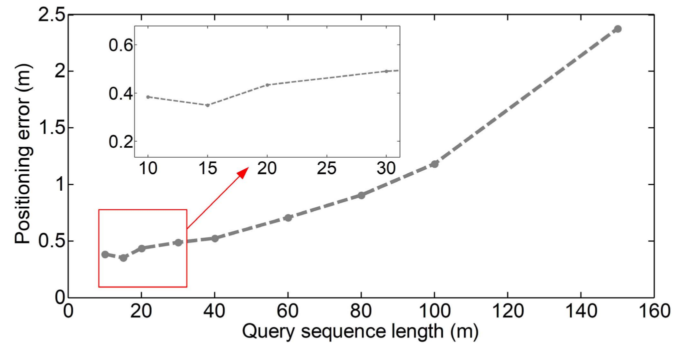

Fig. 10. RMS value of positioning error of MEMS INS aided by matching with respect to the query length.

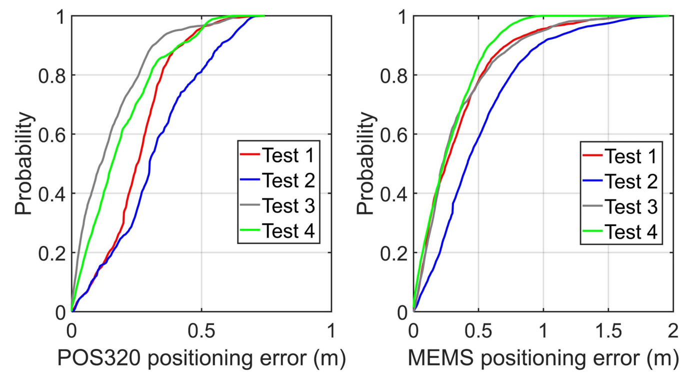

Fig. 11. CDF of the four tests positioning errors. POS320 and MEMS provide the INS measurements. The positioning method is based on INS aided by feature matching.

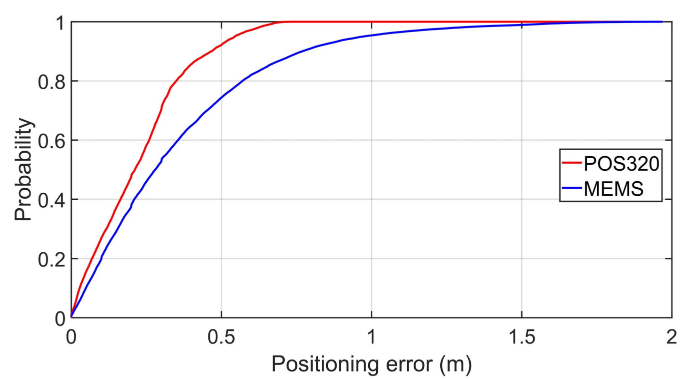

Fig. 12. CDF of the positioning errors by using POS320 and MEMS, respectively. The positioning error is the collection of positioning errors of four tests.

background map plays an important part in accuracy positioning, which provides high-frequency matched positions in time to prevent the inertial solution drifting. It can be indicated that the proposed localization method can maintain the accuracy and stability based on the low-precision MEMS IMU.

As the collection of four positioning errors, Fig. 12 indicates that POS320 and MEMS aided by matching can achieve 0.6-m positioning accuracy with 97.26% confidence and 1-m positioning accuracy with 95.39% confidence, respectively. In the literature [12], the authors presented and compared the positioning accuracy of different conventional mainstream onboard navigation methods for train localization. That work showed that, when the GNSS-blocked period lasts 90 s, the maximum positioning errors of the GNSS/INS integrated system, the GNSS/INS/odometer integrated system, and the LiDAR-aided hybrid integrating system were 17, 10, and 5 m, respectively. Jiang *et al.* reported in a previous study [46] that the GNSS/INS/odometer/map-matching train localization system can maintain a positioning accuracy of 1.5 m during 300-s GNSS outage time. Wang *et al.* [7] proposed a train positioning method based on vision and millimeter-wave radar data fusion, and its positioning error is less than 5 m. As mentioned above, our proposed method uses only an onboard INS aided by matching that can work independently and maintain a positioning accuracy of 1 m without GNSS. Comparing our results with those reported in the state-of-the-art approaches, we can conclude that the proposed train localization method performs better in terms of positioning accuracy. The proposed train positioning method is able to enhance the robustness and accuracy of the multisensory train positioning system.

V. Conclusion

This article presented a train positioning approach by matching a new kind of rail feature, the track irregularity. By using onboard INS, these unique, continuous, and location-relevant track feature information can be sensed, and INS attitude measurement responses to the track irregularity are regarded as a track signature for the feature matching locating process. INS aided by the track irregularity matching can achieve independent, high-precision, and reliable navigation under signal disturbance environment. The proposed train localization method mainly contains coarse positioning, feature matching, and data fusion. INS provides a coarse position and track signature sequence for feature matching. After the feature matching process, the matched position works as an external observation update to prevent inertial solution drifting, and the optimal estimation position can be obtained. Field tests are conducted to assess the performance of the positioning method. The results indicate that a typical tactical-grade IMU can achieve an accuracy of 0.6 m with 97.26% confidence, and the rms value of positioning error is less than 0.24 m based on this proposed locating system. Meanwhile, a 1-m positioning accuracy with 95.39% confidence is achieved when using an MEMS IMU, which can significantly benefit the multisensory train positioning system in improving its accuracy, robustness, and reliability.

Train positioning is a complicated problem regarding accuracy, robustness, and reliability. In this research, we concentrate on validating the newly proposed method and assessing its performance initially, while some other key topics on this issue are worth noting and would be studied in detail in future work. For feature matching, the predefined feature map update is necessary. For future work, more types of map creation and update methods, such as crowd-sourced databases, SLAM, will be explored for field applications.

VI. Acknowledgment

The authors would like to thank Dr. H. Tang in our group for providing the MEMS in the field test.

References

[1] W. Jiang, D. Liu, B. Cai, C. Rizos, J. Wang, and W. ShangGuan, "A fault-tolerant tightly coupled GNSS/INS/OVS integration vehicle navigation system based on an FDP algorithm," *IEEE Trans. Veh. Technol.*, vol. 68, no. 7, pp. 6365–6378, Jul. 2019.

[2] M. Lauer and D. Stein, "A train localization algorithm for train protection systems of the future," *IEEE Trans. Intell. Transp. Syst.*, vol. 16, no. 2, pp. 970–979, Apr. 2015.

[3] D. Liu, W. Jiang, B. Cai, J. Wang, and W. Shangguan, "A tightly-coupled GNSS/INS/MM integrated system based on binary search algorithm for train localization applications," in *Proc. 32nd Int. Tech. Meeting Satell. Division Inst. Navigat. (ION GNSS+)*, Oct. 2019, pp. 1272–1283.

[4] M. Obst, C. Adam, G. Wanielik, and R. Schubert, "Probabilistic multipath mitigation for GNSS-based vehicle localization in urban areas," in *Proc. I_{ON} GNSS Conf.*, 2012, pp. 1454–1461.

[5] O. Heirich, "Bayesian train localization with particle filter, loosely coupled GNSS, IMU, and a track map," *J. Sensors*, vol. 2016, no. 12, pp. 1–15, Mar. 2016, Art. no. 2672640.

[6] S. Damy, "A novel GNSS-based positioning system to support railway operations," Ph.D. dissertation, Imperial College London, London, U.K., 2016.

[7] Z. Wang, G. Yu, B. Zhou, P. Wang, and X. Wu, "A train positioning method based-on vision and millimeter-wave radar data fusion," *IEEE Trans. Intell. Transp. Syst.*, early access, Feb. 3, 2021, doi: 10.1109/TITS.2020.3046497.

[8] J. Otegui, A. Bahillo, I. Lopetegi, and L. E. Diez, "A survey of train positioning solutions," *IEEE Sensors J.*, vol. 17, no. 20, pp. 6788–6797, Aug. 2017.

[9] J. Otegui, A. Bahillo, I. Lopetegi, and L. E. Diez, "Evaluation of experimental GNSS and 10-DOF MEMS IMU measurements for train positioning," *IEEE Trans. Instrum. Meas.*, vol. 68, no. 1, pp. 269–279, Jan. 2019.

[10] B. Cai, B. Wu, and D. Lu, "Survey of performance evaluation standardization and research methods on GNSS-based localization for railways," *Chin. J. Electron.*, vol. 29, no. 1, pp. 22–33, Jan. 2020.

[11] W. Jiang, S. Chen, B. Cai, J. Wang, W. ShangGuan, and C. Rizos, "A multi-sensor positioning method-based train localization system for low density line," *IEEE Trans. Veh. Technol.*, vol. 67, no. 11, pp. 10425–10437, Nov. 2018.

[12] W. Jiang *et al.*, "A seamless train positioning system using a LiDAR-aided hybrid integration methodology," *IEEE Trans. Veh. Technol.*, vol. 70, no. 7, pp. 6371–6384, Jul. 2021.

[13] S. S. Saab, "A map matching approach for train positioning. I. Development and analysis," *IEEE Trans. Veh. Technol.*, vol. 49, no. 2, pp. 467–475, Mar. 2000.

[14] S. S. Saab, "A map matching approach for train positioning. II. Application and experimentation," *IEEE Trans. Veh. Technol.*, vol. 49, no. 2, pp. 476–484, Mar. 2000.

[15] K. Harada, Y. Maki, K. Ishiguri, and A. Kazato, "Development of train positioning system using track curvature collation applied with spatial filtering," *Quart. Rep. RTRI*, vol. 61, no. 3, pp. 178–183, 2020.

[16] K. Gerlach and C. Rahmig, "Multi-hypothesis based map-matching algorithm for precise train positioning," in *Proc. Int. Conf. Inf. Fusion*, 2009, pp. 1363–1369.

[17] O. Heirich, A. Lehner, P. Robertson, and T. Strang, "Measurement and analysis of train motion and railway track characteristics with inertial sensors," in *Proc. 14th Int. IEEE Conf. Intell. Transp. Syst. (ITSC)*, Oct. 2011, pp. 1995–2000.

[18] O. Heirich, P. Robertson, A. C. Garcia, and T. Strang, "Bayesian train localization method extended by 3D geometric railway track observations from inertial sensors," in *Proc. 15th Int. Conf. Inf. Fusion*, 2012, pp. 416–423.

[19] T. Daoust, F. Pomerleau, and T. D. Barfoot, "Light at the end of the tunnel: High-speed LiDAR-based train localization in challenging underground environments," in *Proc. 13th Conf. Comput. Robot Vis. (CRV)*, Jun. 2016, pp. 93–100.

[20] O. Heirich, B. Siebler, and E. Hedberg, "Study of train-side passive magnetic measurements with applications to train localization," *J. Sensors*, vol. 2017, pp. 1–10, Jun. 2017.

[21] E. Hedberg and M. Hammar, "Train localization and speed estimation using on-board inertial and magnetic sensors," M.S. thesis, Dept. Elect. Eng., Linkoping Univ., Linköping, Sweden, 2015.

[22] B. Siebler, O. Heirich, S. Sand, and U. D. Hanebeck, "Joint train localization and track identification based on Earth magnetic field distortions," in *Proc. IEEE/ION Position, Location Navigat. Symp. (PLANS)*, Apr. 2020, pp. 941–948.

[23] O. Heirich, A. Steingass, A. Lehner, and T. Strang, "Velocity and location information from onboard vibration measurements of rail vehicles," in *Proc. 16th Int. Conf. Inf. Fusion*, 2013, pp. 1835–1840.

[24] O. Heirich, "Localization of trains and mapping of railway tracks," Ph.D. dissertation, Dept. Elect. Comput. Eng., Technische Universität München, Munich, Germany, 2020.

[25] Y. Wang, P. Wang, X. Wang, and X. Liu, "Position synchronization for track geometry inspection data via big-data fusion and incremental learning," *Transp. Res. C, Emerg. Technol.*, vol. 93, pp. 544–565, Aug. 2018.

[26] Z. Gao, M. Ge, Y. Li, W. Shen, H. Zhang, and H. Schuh, "Railway irregularity measuring using Rauch–Tung–Striebel smoothed multi-sensors fusion system: Quad-GNSS PPP, IMU, odometer, and track gauge," *GPS Solutions*, vol. 22, no. 2, p. 36, 2018.

[27] A. J. Dean, "Terrain-based road vehicle localization using attitude measurements," Ph.D. dissertation, College Eng., Pennsylvania State Univ., State College, PA, USA, 2008.

[28] A. Dean, R. Martini, and S. Brennan, "Terrain-based road vehicle localisation using particle filters," *Veh. Syst. Dyn.*, vol. 49, no. 8, pp. 1209–1223, 2011.

[29] Q. J. Chen *et al.*, "A railway track geometry measuring trolley system based on aided INS," *Sensors*, vol. 18, no. 2, 2018, p. 538.

[30] Q. Chen, X. Niu, Q. Zhang, and Y. Cheng, "Railway track irregularity measuring by GNSS/INS integration," *Navigation*, vol. 62, no. 1, pp. 83–93, Mar. 2015.

[31] F. Zhu, W. Zhou, Y. Zhang, R. Duan, X. Lv, and X. Zhang, "Attitude variometric approach using DGNSS/INS integration to detect deformation in railway track irregularity measuring," *J. Geodesy*, vol. 93, no. 9, pp. 1571–1587, 2019.

[32] P. F. Westeon, C. S. Ling, C. Roberts, C. J. Goodman, P. Li, and R. M. Goodall, "Monitoring vertical track irregularity from in-service railway vehicles," *Proc. Inst. Mech. Eng., F, J. Rail Rapid Transit Inst. Mech. Eng.*, vol. 221, no. 1, pp. 75–88, Jan. 2007.

[33] P. F. Weston, C. S. Ling, C. J. Goodman, C. Roberts, P. Li, and R. M. Goodall, "Monitoring lateral track irregularity from in-service railway vehicles," *Proc. Inst. Mech. Eng., F, J. Rail Rapid Transit*, vol. 221, no. 1, pp. 89–100, Jan. 2007.

[34] S. Karamihas, "Improvement of inertial profiler measurements of urban and low-speed roadways," Ph.D. dissertation, Dept. Mech. Eng., Univ. Michigan, Ann Arbor, MI, USA, 2021.

[35] Q. Chen, X. Niu, J. Kuang, and J. Liu, "IMU mounting angle calibration for pipeline surveying apparatus," *IEEE Trans. Instrum. Meas.*, vol. 69, no. 4, pp. 1765–1774, Apr. 2020.

[36] N. El-Sheimy, H. Hou, and X. Niu, "Analysis and modeling of inertial sensors using Allan variance," *IEEE Trans. Instrum. Meas.*, vol. 57, no. 1, pp. 140–149, Jan. 2008.

[37] E. H. Shin, "Estimation techniques for low-cost inertial navigation," Ph.D. dissertation, Dept. Geomatics Eng., Calgary Univ., Calgary, AB, Canada, 2005.

[38] P. D. Groves, *Principles of GNSS, Inertial, and Multisensor Integrated Navigation Systems*. Fitchburg, MA, USA: Artech House, 2013.

[39] X. Niu *et al.*, "Development and evaluation of GNSS/INS data processing software for position and orientation systems," *Surveys Rev.*, vol. 47, no. 341, pp. 87–98, 2015.

[40] Y. Zhou, Q. Chen, and X. Niu, "Kinematic measurement of the railway track centerline position by GNSS/INS/odometer integration," *IEEE Access*, vol. 7, pp. 157241–157253, 2019.

[41] Y. Wu, "RodFIter: Attitude reconstruction from inertial measurement by functional iteration," *IEEE Trans. Aerosp. Electron. Syst.*, vol. 54, no. 5, pp. 2131–2142, Feb. 2018.

[42] Y. Wu and G. Yan, "Attitude reconstruction from inertial measurements: QuatFIter and its comparison with RodFIter," *IEEE Trans. Aerosp. Electron. Syst.*, vol. 55, no. 6, pp. 3629–3639, Dec. 2019.

[43] Y. Wu, "INavFIter: Next-generation inertial navigation computation based on functional iteration," *IEEE Trans. Aerosp. Electron. Syst.*, vol. 56, no. 3, pp. 2061–2082, Jun. 2020.

[44] E. H. Shin, "Accuracy improvement of low cost INS/GPS for land applications," M.S. thesis, Dept. Geomatics Eng., Calgary Univ., Calgary, AB, Canada, 2002.

[45] Q. Chen, Q. Zhang, X. Niu, and Y. Wang, "Positioning accuracy of a pipeline surveying system based on MEMS IMU and odometer: Case study," *IEEE Access*, vol. 7, pp. 104453–104461, 2019.

[46] W. Jiang, S. Chen, B. Cai, C. Rizos, J. Wang, and W. ShangGuan, "An analysis of PPP-GPS-based decentralized train multi-sensor navigation system," *GPS Solutions*, vol. 24, no. 3, pp. 1–14, Jul. 2020.

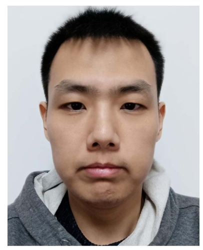

Yukun Zhou received the B.E. degree in surveying and mapping Engineering from Center South University, Changsha, China, in 2016, and the M.E. degree in geodesy and survey engineering from Wuhan University, Wuhan, China, in 2019, where he is currently pursuing the Ph.D. degree with the GNSS Research Center.

His research interests include INS and its applications in precise surveying engineering of railway track and train localization.

Qijin Chen received the B.Eng. and Ph.D. degrees in geodesy and survey engineering from Wuhan University, Wuhan, China, in 2011 and 2016, respectively.

He is currently an Associate Research Fellow with the GNSS Research Center, Wuhan University. His research interests include INS with aiding and its applications in geodesy and precise surveying engineering including railway track geometry measuring and underground pipeline surveying.

Rongsheng Wang has 20 years of experience in railway track daily maintenance and trackside equipment detection. He is currently with Fuyang Public Works Station, China Railway Shanghai Group Company, Ltd., Fuyang, China. He is also the Director General of Fuyang Public Works Station and In Charge of the inspection and maintenance of five railway lines and trackside equipment detection.

Guiliang Jia has ten years of experience in railway track daily maintenance and trackside equipment detection. He is currently with Fuyang Public Works Station, China Railway Shanghai Group Company, Ltd., Fuyang, China. He is also the Deputy Director General of Fuyang Public Works Station and In Charge of the track inspection and maintenance of five railway lines. He is also an expert in the precise measurement of railway tracks and track irregularity inspection.

Xiaoji Niu received the B.Eng. and Ph.D. degrees from the Department of Precision Instruments, Tsinghua University, in 1997 and 2002, respectively.

He did his Post-Doctoral Research with the University of Calgary. He was a Senior Scientist with SiRF Technology Inc. He is currently a Professor with the GNSS Research Center, Wuhan University, China. He has authored or coauthored more than 90 academic articles. He leads the Multi-Sensor Navigation Group focuses on GNSS/INS integrations, low-cost navigation sensor fusion, and its new applications.